Supporting Information

Strategic harmonization of silica shell stabilization with Pt embedding on AuNPs for efficient artificial photosynthesis

Dinesh Kumar[a,*], *Chan Hee Park*[b,*] *and Cheol Sang Kim*[a,b,*]

[a]Department of Bionanosystem Engineering, Graduate School, Jeonbuk National University, Jeonju 561-756, South Korea.

[b]Department of Mechanical Design Engineering, Jeonbuk National University, Jeonju 561-756, South Korea.

This PDF include experimental details, table (S1), figures (S1-S13), and references.

1. General

All chemical reagents were purchased from Sigma-Aldrich (St. Louis, MO, USA) and used as received without further purification. HR-TEM (JEOL-2010, Japan, 200 kV) was used for HRTEM analysis. Extinction spectra were obtained with a UV spectrometer (SCINCO, South Korea). Structural analyses were performed using X-ray diffraction (Rigaku D/MAX 2500Tokyo, Japan). The BET (Brunauer-Emmett-Teller) surface area measurement and BJH (Barrett-Joyner-Halenda) adsorption-desorption cumulative surface area measurement analysis of pores have been performed on Micromeritics ASAP 2020 instrument. The amount of CO_2 dissolved in the reaction samples was determined using an HI 3818 carbon dioxide test kit (Hanna Instruments, Romania). ^{1}H-NMR and ^{13}C-NMR analyses were carried out using a JEOL JNM AL-400 instrument. The GC-MS analysis was carried out on Agilent 7890A GC and Agilent 5975C mass selective detector (Agilent Technologies, Santa Clara, CA, USA). Fourier transform infrared (FT-IR) spectra were recorded on a Jasco FTIR-4200 spectrophotometer (Maryland, USA). Renishaw, Raman micro system 2000 (Derbyshire, England) was used for the Raman analysis. A Xe lamp (Ceramaxs, Waltham, USA) with a power density of 6 W/cm^2 was used as a visible light (390-770 nm) source (Figure S3). In addition, a near-infrared (NIR) laser (OCLA Laser, Passive Cooled InGaAs diode laser, LaserLab® South Korea, 808 nm, output power = 1-15 W) was used. A solar simulator (Newport) with a power density of 0.23 W/cm^2 was used.

2. Methods

2.1. Preparation of gold nanospheres

The spherical shaped AuNPs (λ_{max} = 528 nm) with average particle aize of 30 nm were synthesized utilizing citrate-modified method.[1, 2] To the boiling solution of $HAuCl_4$ (0.5mM, 50 mL), 1.1 mL of 38.8 mM sodium citrate solution was added with continuous vigorous stirring. After that the resulting mixture was refluxed for 30 min for complete reduction of $HAuCl_4$ to AuNPs as the color turned from light yellow to wine red. Finally, the final reaction product was centrifuged at 8000 rpm and the resulting 30 nm sized nanoparticles were re-dispersed in distilled water for further use.

2.2. Preparation of AuNSs

The synthesis of AuNSs (λ_{max} = 669 nm, 30 nm) was carried out by following previously reported method.[3] In a typical experiment, 20 mL of HEPES (100 mM, pH 7.4) solution was mixed with 30 mL of deionized water, followed by the addition of 500 µL of $HAuCl_4$ (20 mM) solution. The resulting mixture was kept undisturbed for 30 min, the color of solution changed from light yellow to slightly purple and finally to greenish blue.

2.3. Preparation of CTAB modified AuNRs

Cetyltrimethyl ammonium bromide (CTAB) mediated growth method was used to prepare AuNRs (λ_{max} = 721 nm, 30 nm).[4] $HAuCl_4$ (0.25 mL, 0.01 M) was mixed with a CTAB aqueous solution (9.75 mL, 0.1 M) to make seed solution. The solution color changed from yellow to pale-brown while ice-cold solution of $NaBH_4$ (600 µL, 0.01 M) was quickly added with vigorous stirring. Then this seed solution was stored in a water bath for 3 h at 28 °C. Growth solution was prepared by mixing CTAB (475 mL, 0.1 M) with $HAuCl_4$ (20 mL, 0.01 M), $AgNO_3$ (3.0 mL, 0.01 M), and ascorbic acid (3.2 mL, 0.1 M) in slow stirring. With the addition of ascorbic acid, the yellow colored solution became colorless. At last, the seed solution (3.6 mL) was quickly added to the growth solution and mixed with brief shaking for 5 s, and then the resulting solution was kept undisturbed in a water bath at 28 °C for 12 h.

2.4. One-pot synthesis of SiO_2 coated gold nanostructures

In the first step, 10 mL of AuNPs (O.D. = 2.0) were mixed with 500 µL of cetyltrimethylammonium bromide (0.1 M) and stirred for 3 h at room temperature. Then, 50 µL of NaOH solution (0.1 M) was added and stirred for another 15-20 min. Lastly, 2 mL of tetraethyl orthosilicate (TEOS) solution (20 µL TEOS + 8 mL distilled water) was added drop

wise and the resulting mixture was stirred overnight. After that, the resultant mixture (AuNPs@SiO_2) was washed twice with ethanol and re-dispersed in 10 mL of ethanol. TEM analysis suggested that 8-10 nm layer of SiO_2 has been formed on AuNPs (Figure S3B, supporting information). To increase the silica shell thickness to 15 nm and 20 nm, the 7 mL and 5 mL of AuNPs (O.D. =2.0) used, respectively (Figure S3C and S3D, supporting information). For less silica shell thickness like 5 nm, 15 mL of AuNPs (O.D. =2.0) were used (Figure S3A, supporting information). For higher silica shell thickness amount of TEOS solution increased relatively. The way of TEOS solution addition is most important in order to vary the thickness of silica shell. The direct (in one go) addition of TEOS solution was not suitable to control the thickness of silica shell as addition of 2 mL to 6 mL of TEOS solution resulted in same silica shell thickness of 10-12 nm (Figure S4, supporting information). Same method was used to coat AuNSs (gold nanostars) and AuNRs (gold nanorods). Though, in case of AuNRs 3 times less amount of TEOS solution was used.

2.5. Preparation of AuNPs@Pt nanoparticles

Pt nanoparticles (2-3 nm) decorated AuNPs were prepared by adding ascorbic acid (1.2 mL) to the AuNPs solution (20 mL, O.D. = 1.0), along with 180 µL of 0.01 M $H_2PtCl_6 \cdot 6H_2O$ and 180 µL of 0.01 M HCl. After addition, the reaction mixture was placed undisturbed for 12 h at 28 °C, and then centrifuged (8000 rpm/15 min) and re-dispersed in distilled water (20 mL).

2.6. Preparation of Pt-AuNPs@SiO_2 nanoparticles

Pt nanoparticles (2-3 nm) were decorated uniformly on AuNPs@SiO_2, by adding ascorbic acid (1.2 mL) to the APS modified AuNPs@SiO_2 nanoparticles solution (20 mL, O.D. = 1.0), along with 180 µL of 0.01 M $H_2PtCl_6 \cdot 6H_2O$ and 180 µL of 0.01 M HCl. After addition, the reaction mixture was placed undisturbed for 12 h at 28 °C, and then centrifuged (7000 rpm/15 min) and resulted nanoparticles (Pt-AuNPs@SiO_2) re-dispersed in distilled water (20 mL). There is a red shift in the UV spectrum from 528 nm (black line) to 540 nm (red line) as AuNPs were coated with SiO_2 shell (AuNPs@SiO_2, Figure S2G) and further red shift from 540 to 553 nm (blue line) was observed as PtNPs were decorated over AuNPs@SiO_2 (Figure 2B).

2.7. Photo-conversion of CO_2

In a typical photo-conversion reaction of CO_2, the nanoparticles solution (10 mL, OD at 553 nm = 1.0) was placed in a Pyrex glass reactor (window diameter = 10 mm) equipped with a water circulation jacket to maintain the reaction temperature at room temperature. Then, the CO_2 was purged in to nanoparticles solution for 30 min to saturation (0.24 mg/mL). A Xe lamp (power density: 6 W/cm^2) was used for visible light irradiation whereas 808 nm laser (3 W/ cm^2) has been used as a source of NIR light irradiation.

2.8. HCOOH formation under H_2 gas reaction with CO_2

Formic acid formation through CO_2 reduction without light irradiation was carried out in the presence of a continuous flow of H_2 for 5 h. H_2 gas was produced by the addition of an aluminum foil to NaOH solution (200 mL, 2.0 M).[5] The as-generated H_2 gas was flowed into CO_2 saturated distilled water constantly for 5 h. Then, after the completion of reaction the pH was adjusted to 12.0 with dilute NaOH and the resulting solution was rotary evaporated to dryness. The final product was analyzed by ^{1}H-NMR and ^{13}C-NMR.

2.9. CO_2 photo-conversion reaction product analysis

After the completion of reaction (5 h) the resulted reaction mixture was centrifuged at 15,000 rpm/15 min to remove nanoparticles and to obtain the supernatant containing product. Then the solution was analyzed with gas chromatography-mass spectrometry (GC-MS). For GC analysis, the oven temperature was varied from 35 °C to 100 °C using helium gas as the carrier gas with an injector temperature of 200 °C and a sampling time of 20 min for GC-MS analysis. The equation obtained from the standard deviation curve was used to calculate the number of moles of formic acid formed.

Also, the pH of resulted reaction mixture was adjusted to 12 by the addition of dilute NaOH solution to convert HCOOH to sodium formate ($HCOO^-Na^+$). After rotary evaporation, the final product was analyzed with ^{1}H-NMR, ^{13}C-NMR (600 MHz, $CDCl_3$), FTIR and Raman spectroscopic studies. The quantum yield (QY) and chemical yield (CY) were calculated using GC and ^{1}H-NMR analysis techniques.

The small aliquots (10 μL) of CO_2 reduction reaction mixtures were placed on a quartz substrate

and allowed to dry and then analyzed for Raman spectroscopy (the samples were analyzed with 532 nm laser excitation (50 mW)). Spectral data was collected over the range 400–1800 cm^{-1} with 10 sec of integration time.

2.10. Chemical and quantum yield calculation

(1) The amount of CO_2 in 10 mL solution was found to be 2.4 mg, as calculated by using a carbon dioxide kit (HI 3818, Hanna Instruments, Romania) and the procedure given along with it. The titration flask was rinsed with a CO_2 purged aqueous sample (5 mL) and 1 drop of phenolphthalein indicator was added. There was no change in the color of the indicator solution was observed. After that, the mixture was titrated with the HI 3818-0 solution provided by the carbon dioxide kit until the emergence of pink color. The total amount consumed for the titration was multiplied by 100 to obtain the quantity (ppm) of CO_2. The experiment was repeated for three times.

(2) The quantification of formic acid was carried out using a standard deviation curve plotted using ^{1}H-NMR (five standard samples of formic acid in $CDCl_3$ with increasing concentrations ranging from 0.015 mM to 0.15 mM) and GC-MS analysis.

(3) The chemical yield was calculated by dividing the molar concentration of formic acid formed by the molar concentration of carbon dioxide dissolved in the reaction sample. For example:
The equation obtained from standard deviation curve (NMR):-
Moles of HCOOH ÷ 10 mL = 0.0001704 M (from standard deviation curve)
Moles of CO_2 ÷ 10 mL = 0.005455 M (calculated using the carbon dioxide kit)
Chemical yield = moles of HCOOH ÷ Moles of CO_2 × 100

$$= 0.0001704 \div 0.005455 \times 100 = 3.12\% \quad (1)$$

The quantum yield of produced formic acid was calculated by using following equation:

QY (%) = number of reacted electrons ÷ number of incident photons × 100%

$$= 2 \times \text{number of formic acid molecules/ number of incident photons} \times 100\% \quad (2)$$

Number of incident photons = moles of $Fe^{2+} \div \phi_\lambda \times t \times F$ (3)

(Moles of Fe^{2+} (calculated) = 0.03588, ϕ_λ = quantum yield of Fe^{2+} ion concentration = 0.65, t = time = 20 s,

F = mean fraction of light absorbed by ferrioxalate solution = 0.1488

Number of incident photons = $0.03588 \div 0.65 \times 20 \times 0.1488$

$= 0.01855$ photons s^{-1} (4)

QY (%) = 2 × number of formic acid molecules/number of incident photons × 100%

$= 2 \times 0.0001704/0.01855 \times 100 = 1.84\%$ (5)

The number of incident photons was measured by the ferrioxalate actinometer method (equations (3) and (4)).[6, 7] The actinometer solution was prepared as follows. In a 100-mL flask, an aqueous solution of $Fe_2(SO_4)_3$ (5 mL, 0.2 M) and an aqueous solution of $K_2C_2O_4$ (5 mL 1.2 M) were added. Then, this mixture was diluted to 100 mL volume by using distilled water. Then, the above actinometer solution (40 mL) was irradiated under visible light for 20 s.

Consequently, the ferrous ion concentration was determined by the formation of the iron-phenanthroline complex, detected by UV-visible spectrophotometry at 510 nm. The analytical procedure was as follows. In a 100-mL flask, the actinometer solution (1 mL) after irradiation, an aqueous solution of 1,10-phenanthroline (2 mL, 0.2 wt %), and a buffer solution (0.5 mL) of pH = 4–5 were mixed and diluted to 100 mL with distilled water, and kept in the dark for 30 min. After 30 min, absorbance of the solution at 510 nm was measured using a UV-visible spectrophotometer. A comparative test was conducted by following the above mentioned procedure for the blank solution (actinometer solution without irradiation), and the ferrous ion concentration was calculated by UV-visible spectrophotometric observation at 510 nm.

Table S1. BET surface area measurement of prepared nanomaterials.

Type of nanoparticles	**BET surface area (m^2/g)**	**BJH Adsorption cumulative surface area of pores (m^2/g)**	**BJH Desorption cumulative surface area of pores (m^2/g)**
AuNPs	3.8571	1.3550	1.8258
AuNPs@SiO_2	4.9660	5.4945	5.9524
Pt-AuNPs@SiO_2	6.2054	3.5490	4.7509

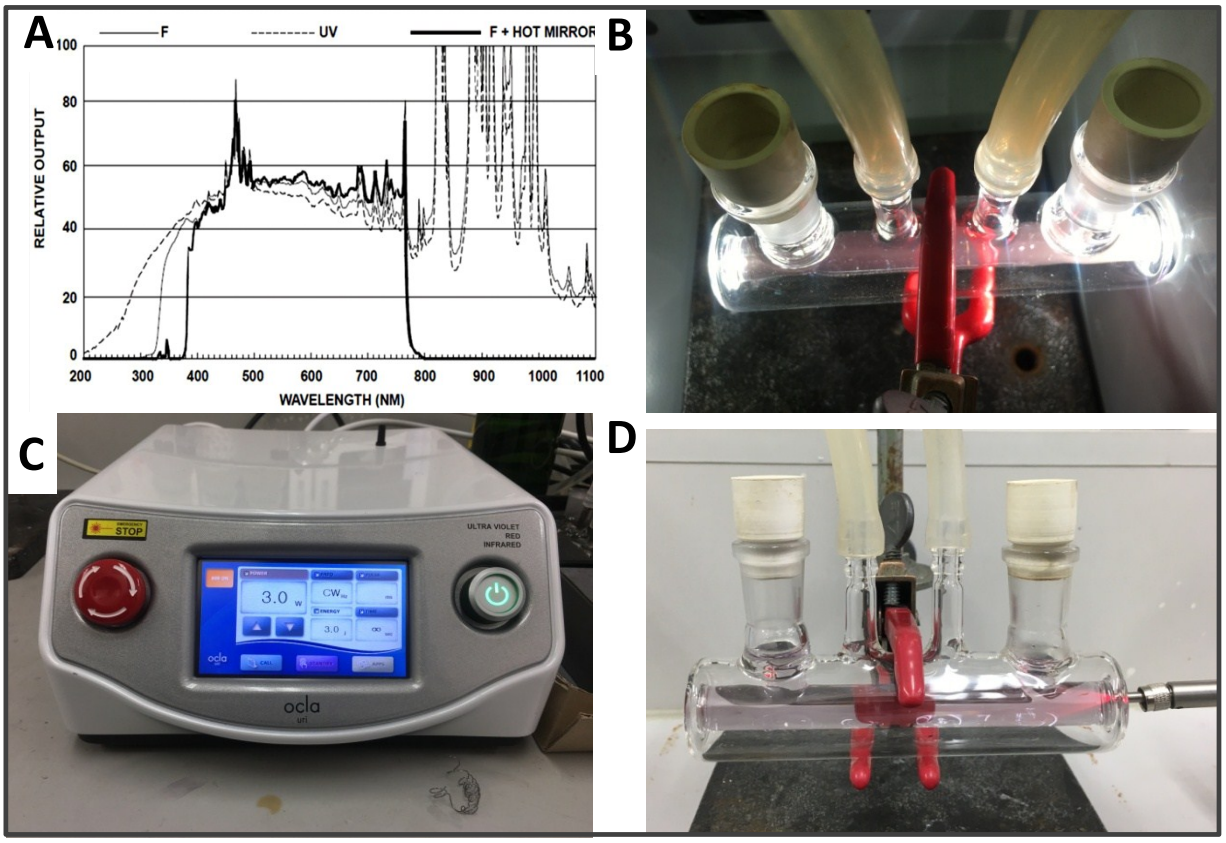

Figure S1. (**A**) Output spectra of Xe lamp (Cermax®, PE300BFA). (**B**) The reactor (Pyrex, 10 ml) with water circulation jacket under visible light. (**B**) NIR (808 nm) laser used for CO_2 photoreduction. (D) NIR light illumination through Pyrex glass reactor.

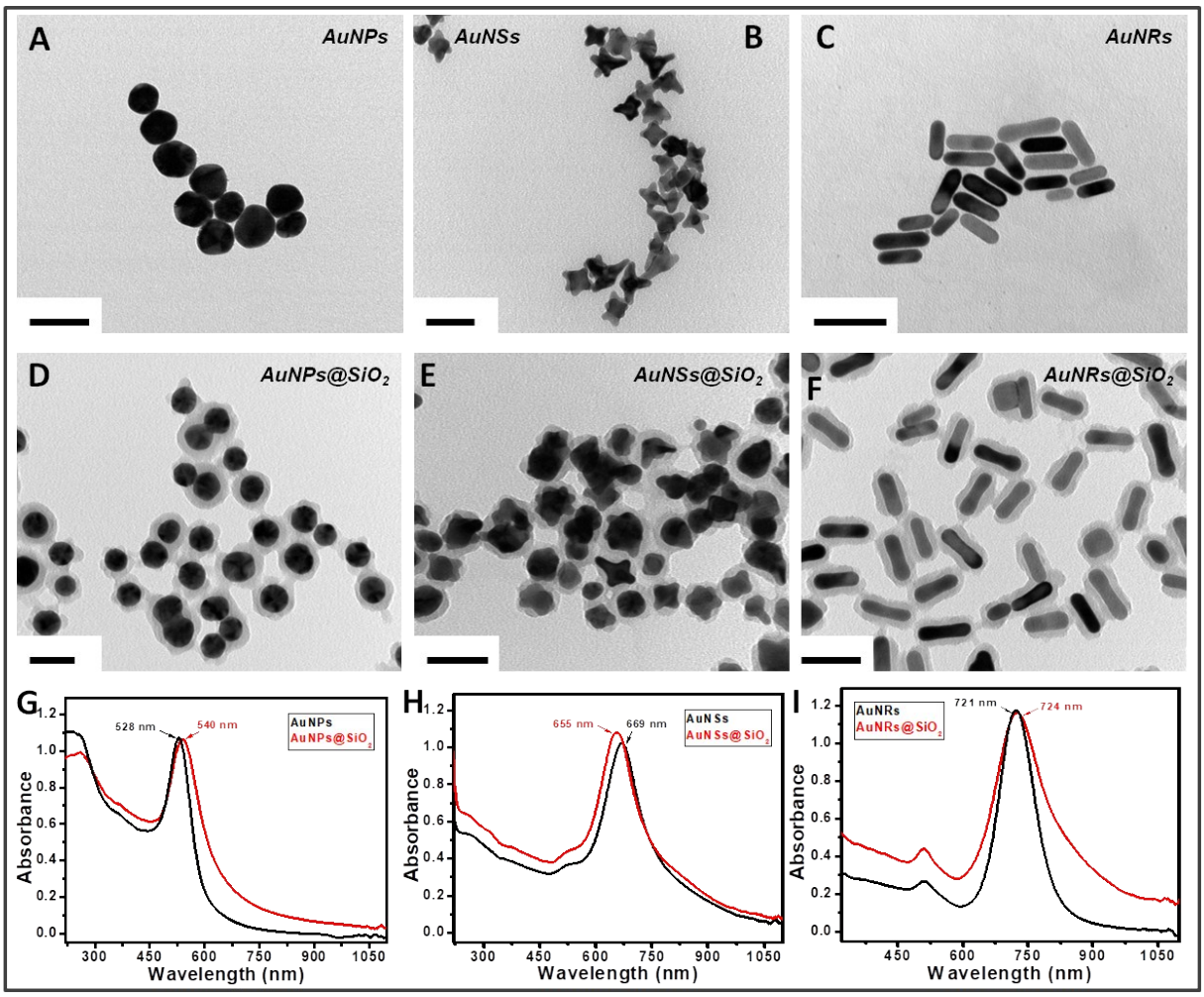

Figure S2. TEM image of (**A**) AuNPs, (**B**) AuNSs, (**C**) AuNRs, (**D**) AuNPs@SiO_2, (**E**) AuNSs@SiO_2, and (**F**) AuNSs@SiO_2 nanoparticles. UV-Visible spectrum of (**G**) AuNPs and AuNPs@SiO_2, (**H**) AuNSs and AuNSs@SiO_2, and (**I**) AuNRs and AuNRs@SiO_2 nanoparticles.

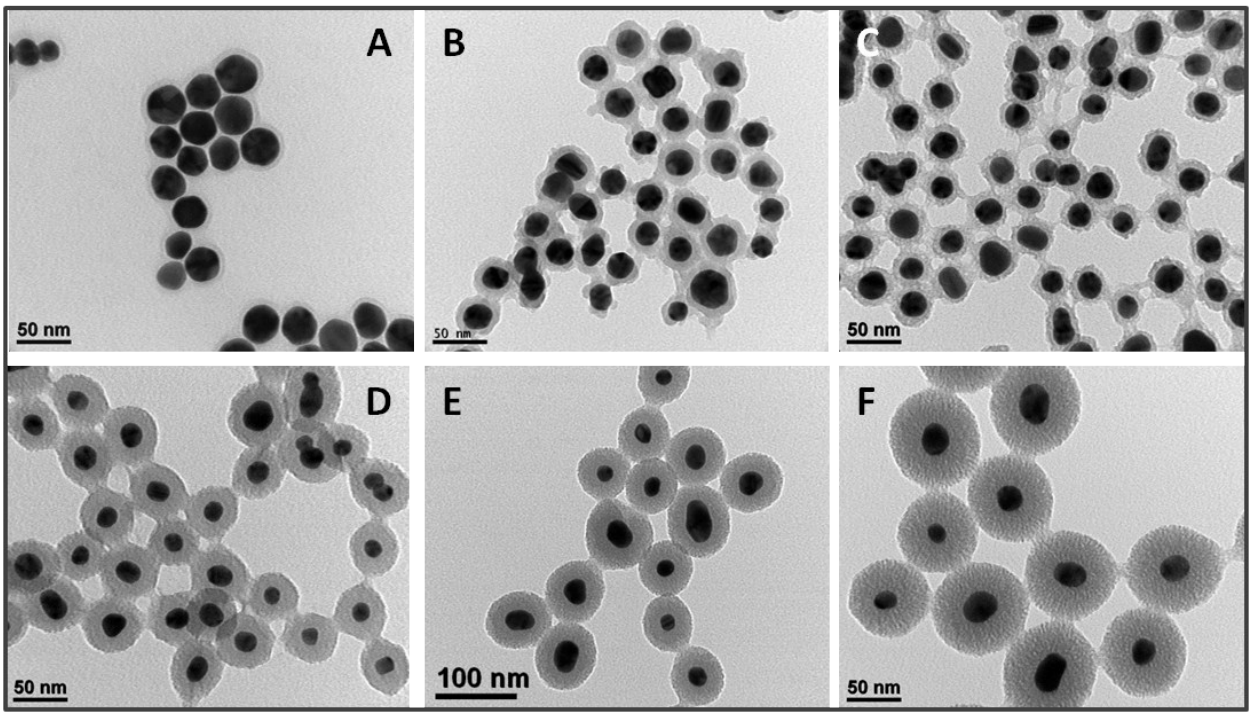

Figure S3. TEM images of AuNPs@SiO_2 nanoparticles with increasing SiO_2 shell thickness such as **(A)** 5 nm, **(B)** 10 nm, **(C)** 15 nm, **(D)** 20 nm, **(E)** 25 nm, and **(F)** 30 nm.

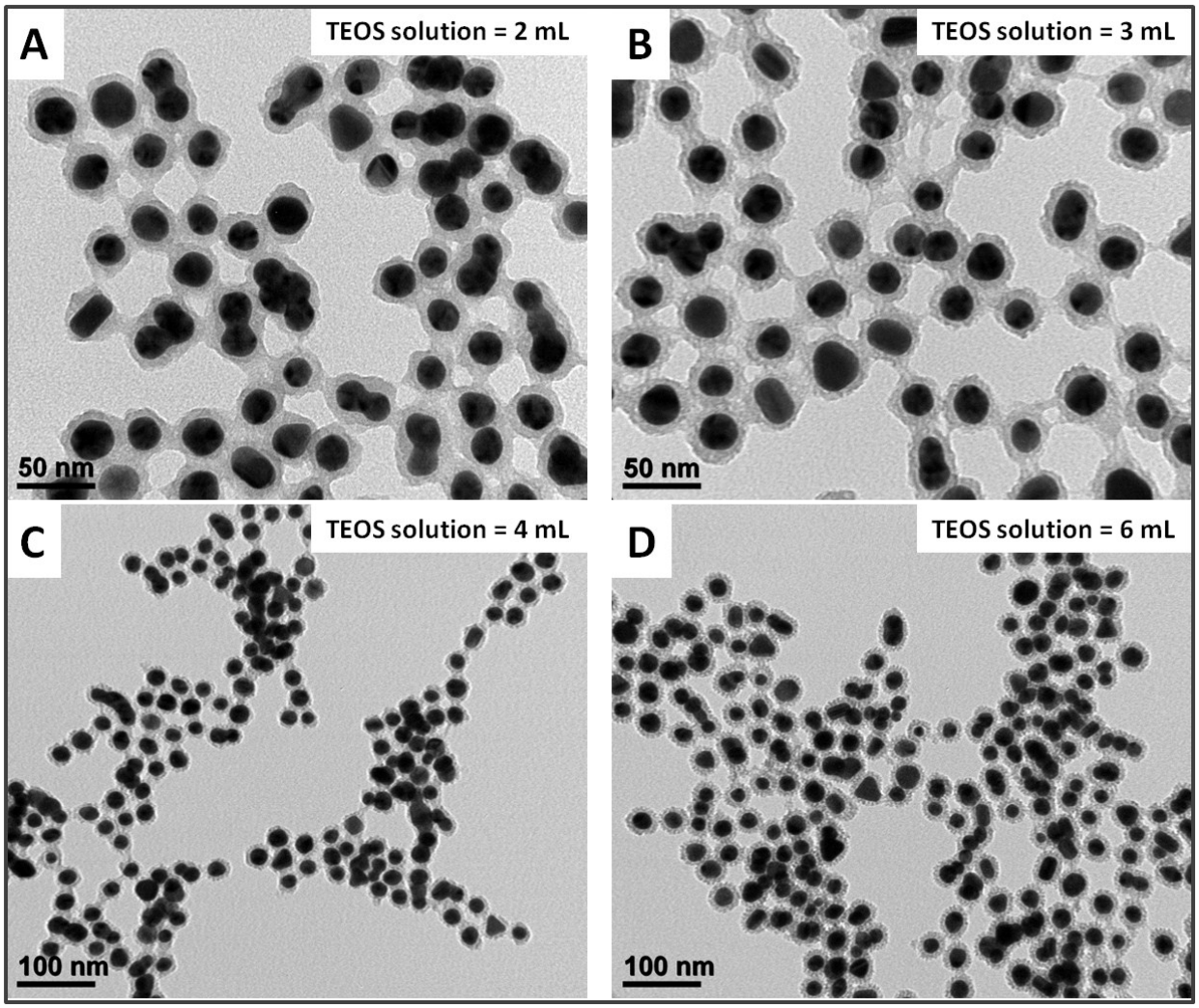

Figure S4. TEM images of AuNPs@SiO_2 nanoparticles with different silica precursor (TEOS) amounts such as (**A**) 2 mL, (**B**) 3 mL, (**C**) 4 mL, and (**D**) 6 mL.

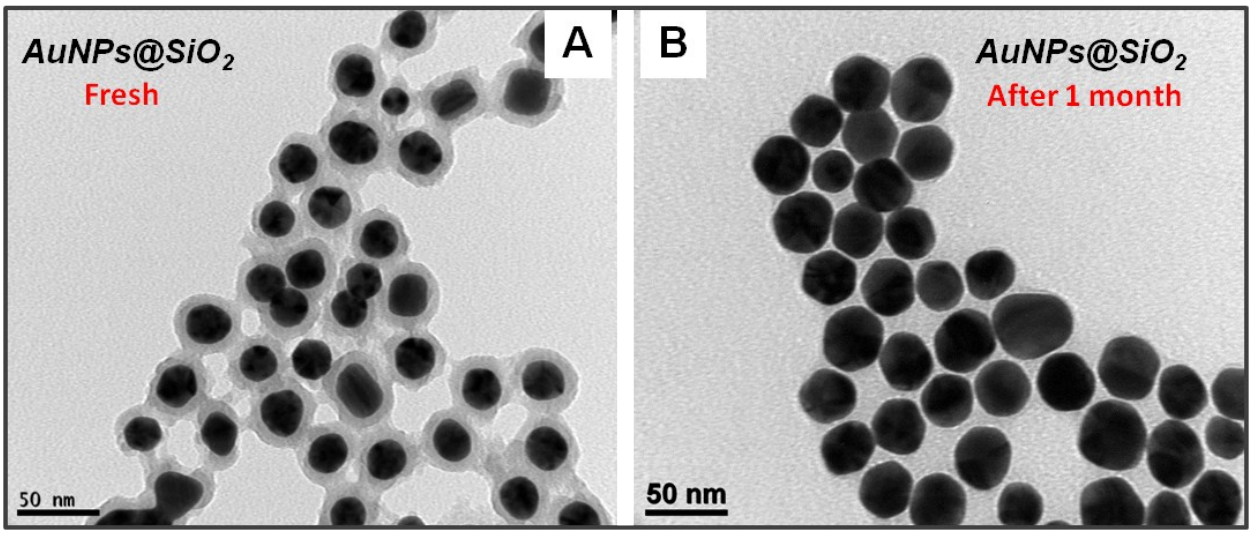

Figure S5. TEM images of AuNPs@SiO_2 nanoparticles **(A)** fresh and same sample **(B)** after 1month.

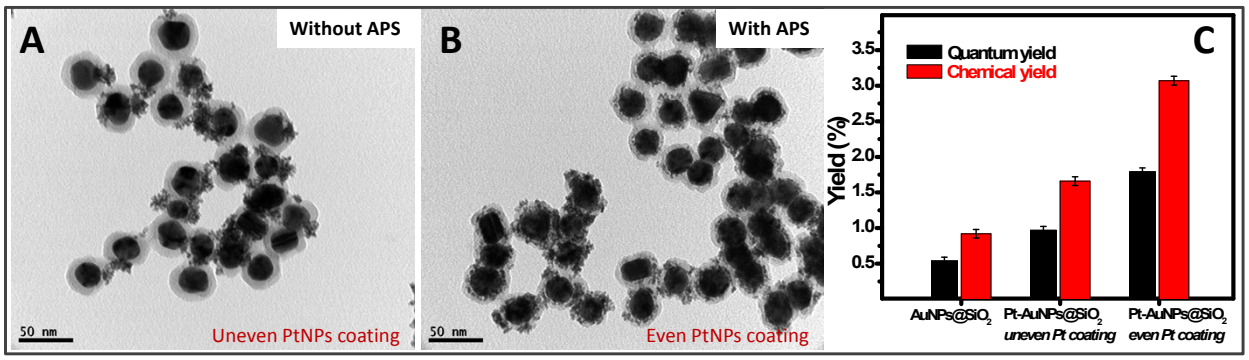

Figure S6. TEM image of **(A)** Pt-AuNPs@SiO_2 nanoparticles with uneven PtNPs coating and **(B)** Pt-AuNPs@SiO_2 nanoparticles with even PtNPs coating. **(C)** Comparative efficiency of AuNPs@SiO_2 nanoparticles, Pt-AuNPs@SiO_2 nanoparticles with uneven PtNPs coating and Pt-AuNPs@SiO_2 nanoparticles with even PtNPs coating for CO_2 photoconversion to HCOOH.

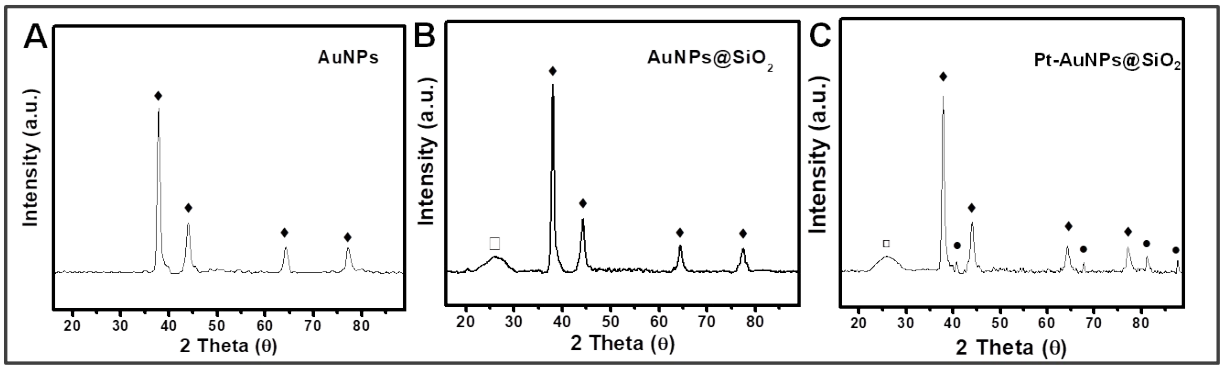

Figure S7. XRD spectrum of **(A)** AuNPs, **(B)** AuNPs@SiO_2, and **(C)** Pt-AuNPs-SiO_2 nanoparticles. (♦= Au, ● = Pt, □ = SiO_2)

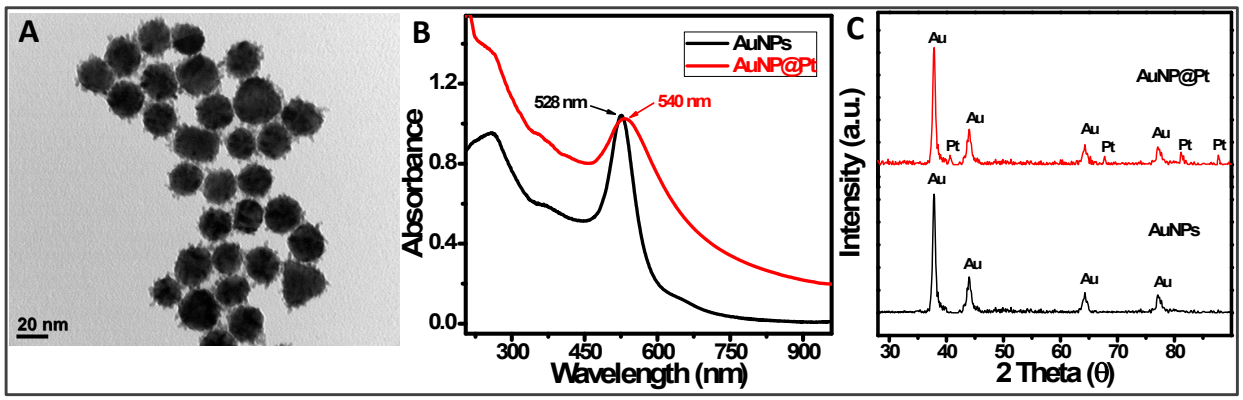

Figure S8. (A) TEM image of AuNP@Pt nanoparticles. **(B)** UV-Visible spectrum and **(C)** XRD patterns of AuNPs and AuNP@Pt nanoparticles.

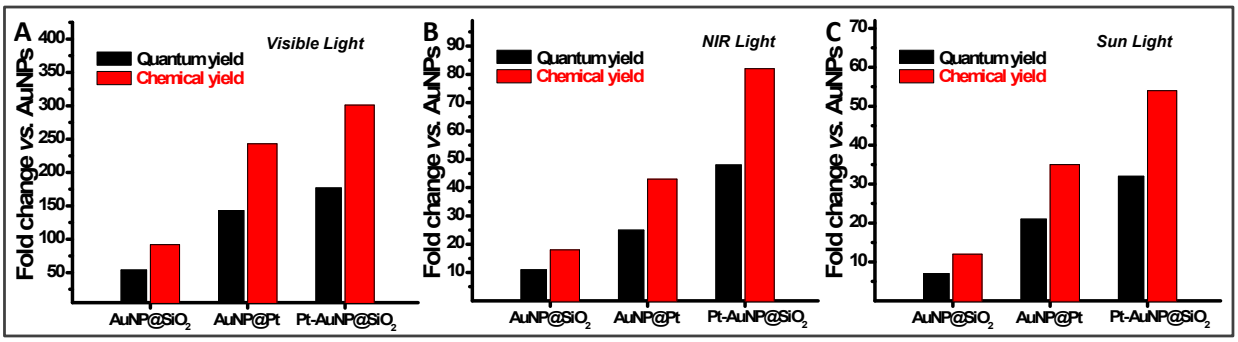

Figure S9. Fold change for the HCOOH formation using AuNPs@SiO_2 AuNPs@Pt, Pt-AuNPs@SiO_2 nanoparticles in comparison to AuNPs in **(A)** visible light **(B)** NIR light and **(C)** sun light irradiation.

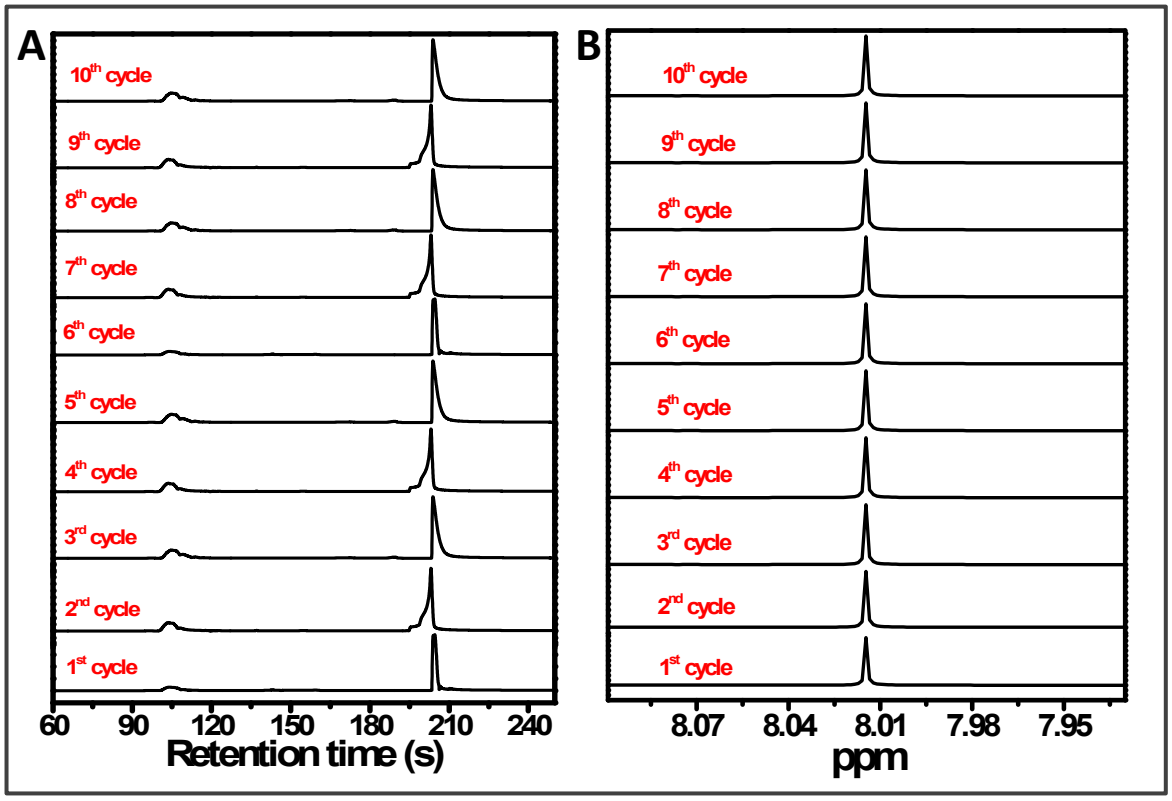

Figure S10. (A) Gas chromatography and **(B)** ^{1}H-NMR spectrums after every Pt-AuNPs@SiO_2 nanoparticles mediated CO_2 reduction recycle in visible light irradiation.

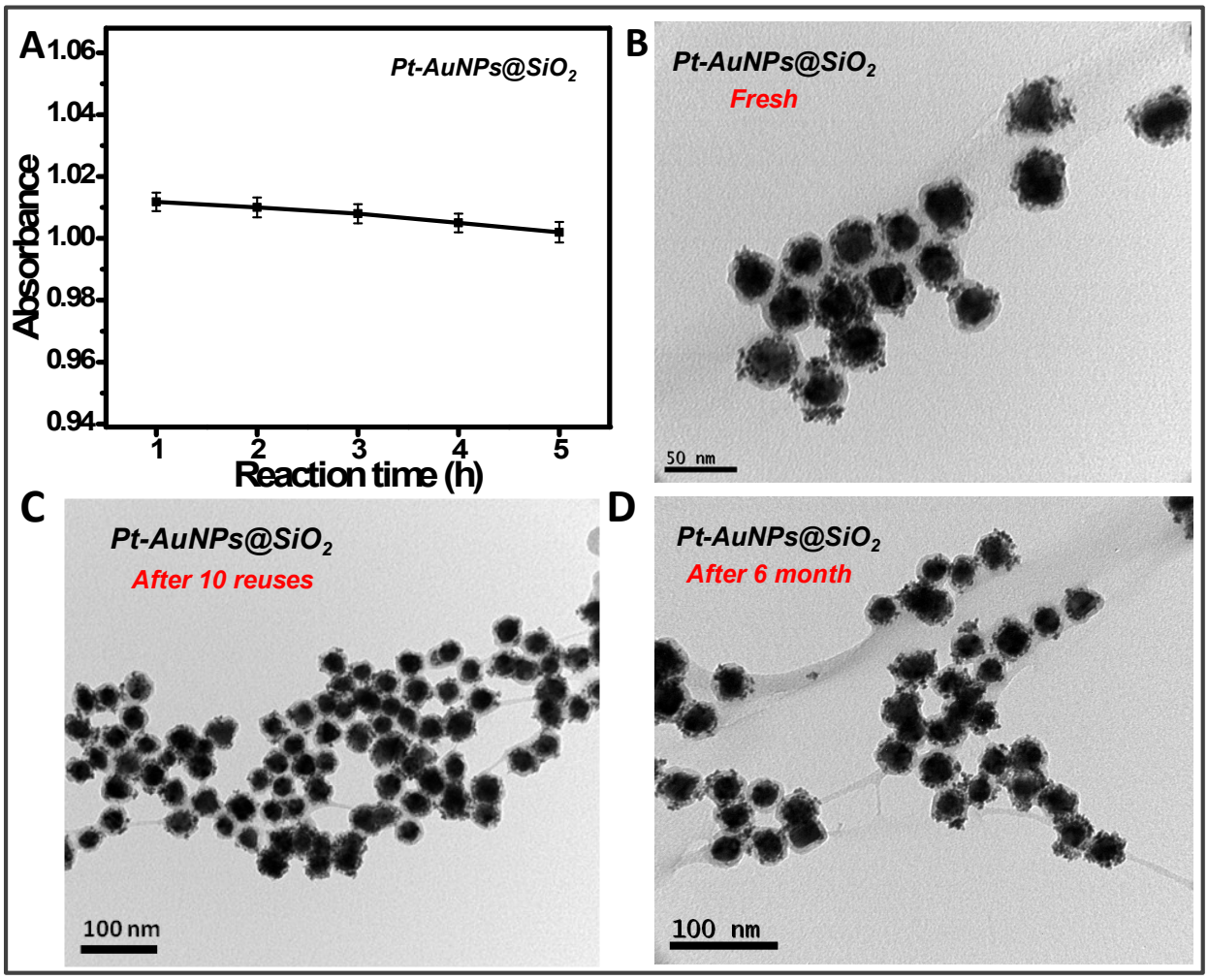

Figure S11. (A) Stability check of Pt-AuNPs@SiO_2 nanoparticles after every recycle using UV-Visible spectroscopy. **(C)** TEM images of Pt-AuNPs@SiO_2 nanoparticles **(A)** fresh and same sample **(B)** after 10 recycles, and **(C)** after 6 months.

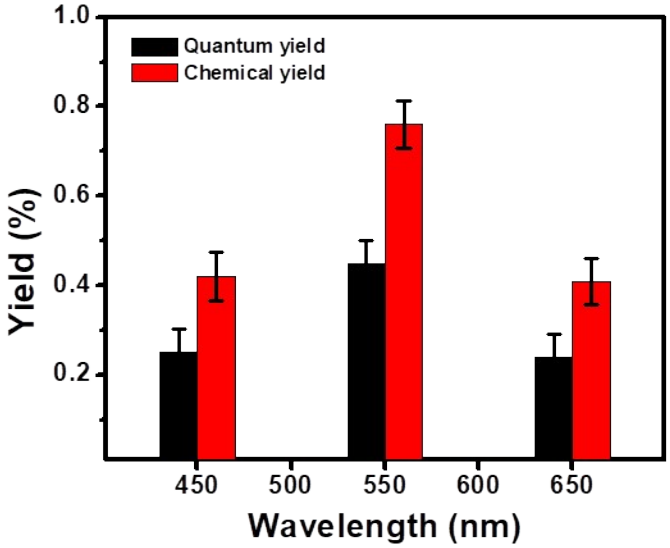

Fig. S12. Quantum yield calculated for the photocatalytic CO_2 reduction to HCOOH using Pt-AuNPs@SiO_2 nanoparticles at three different incident monochromatic wavelengths.

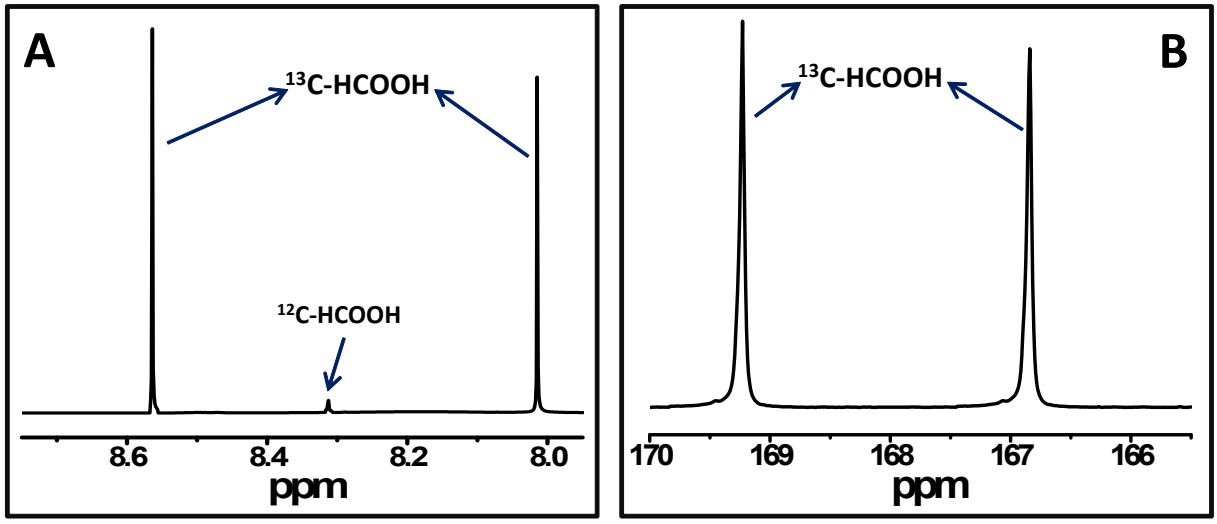

Fig. S13. (A) ^{1}H-NMR spectra and **(B)** ^{13}C-NMR spectra for the HCOOH produced by photocatalytic reduction of isotopic $^{13}CO_2$ gas.

References

1. N. G. Bastús, J. Comenge and V. Puntes, *Langmuir*, 2011, **27**, 11098-11105.
2. F. Pincella, K. Isozaki and K. Miki, *Light Sci Appl*, 2014, **3**, e133.
3. J. Xie, J. Y. Lee and D. I. C. Wang, *Chemistry of Materials*, 2007, **19**, 2823-2830.
4. Z. Ban, Y. A. Barnakov, F. Li, V. O. Golub and C. J. O'Connor, *Journal of Materials Chemistry*, 2005, **15**, 4660-4662.
5. L. Soler, J. Macanás, M. Muñoz and J. Casado, *Journal of Power Sources*, 2007, **169**, 144-149.
6. C. An, J. Wang, W. Jiang, M. Zhang, X. Ming, S. Wang and Q. Zhang, *Nanoscale*, 2012, **4**, 5646-5650.
7. M. Schiavello, V. Augugliaro, V. Loddo, M. J. López-Muñoz and L. Palmisano, *Research on Chemical Intermediates*, 1999, **25**, 213-227.